High-Pressure Acceleration of the Growth Kinetics of Glucose Isomerase Crystals

Yoshihisa Suzuki,*,† Gen Sazaki,‡,§ Takuro Matsui,‡,§ Kazuo Nakajima,‡ and Katsuhiro Tamura†

Department of Chemical Science and Technology, Faculty of Engineering, The University of Tokushima, 2-1 Minamijosanjima, Tokushima 770-8506, Japan, Institute for Materials Research, Tohoku University, 2-1-1 Katahira, Aoba-ku, Sendai 980-8577, Japan, and Center for Interdisciplinary Research, Tohoku University, Aramaki, Aoba-ku, Sendai 980-8578, Japan

Received: August 10, 2004; In Final Form: December 13, 2004

The growth and dissolution rates of glucose isomerase crystals ({1 0 1} face) were measured in situ at 0.1 and 100 MPa. From these data, we determined that the solubilities at 25 °C were $C_e = 3.1 \pm 0.9$ and 2.6 ± 0.5 mg mL^{-1} at 0.1 and 100 MPa, respectively. At the same supersaturation of $\sigma = 2.5$ ($\sigma \equiv \ln(C/C_e)$, $C =$ the concentration of glucose isomerase, $C_e =$ the solubility) and temperature ($T = 25$ °C), the growth rate under 100 MPa was 7.6 times larger than that under 0.1 MPa. This result shows, for the first time, a kinetic acceleration of the growth rates of protein crystals with increasing pressure. The growth rates vs σ data fitted well with a two-dimensional nucleation growth model of a polynucleation type. The fitting results indicate that the acceleration is mainly due to the decrease in the molecular surface energy of the glucose isomerase crystal with pressure.

1. Introduction

X-ray crystallography is the most powerful tool for analyzing the three-dimensional (3D) complex structure of a protein molecule. However, among the steps performed in structural analysis, that of protein crystallization remains a bottleneck. For example, a summary of progress in the Human Proteome Structural Genomics pilot project shows the success rate of getting structure from clone to be about 10% (15 structures from 124 clones).[1,2] The rate-limiting step, evidently, is the production of crystals suitable for X-ray crystallography (19 crystals from 63 purified samples) even after the proteins have been solubilized (89 solubilized samples from 115 expressed samples) and highly purified (63 purified samples from 89 solubilized samples). Without increasing the success rate, we cannot determine the 3D structures of many biologically important protein molecules.

Factors that accelerate the crystallization probably play an important role in solving this problem. In 1990, Visuri et al. found that hydrostatic pressure could be such a factor. They reported that the rate of crystallization (changes in the total mass of the crystals yielded per minute) of glucose isomerase drastically increased with increasing pressure.[3] Subsequently, many studies of the effects of pressure on protein crystallization have been reported.[4−23]

In thermodynamic terms, a positive volume change accompanying the dissolution of protein crystals results in a decrease in its solubility, and hence, an increased supersaturation accelerates crystal growth.[24] Table 1 provides a summary of the effects of pressure on the solubilities of protein crystals for several proteins and crystal forms.

In contrast, considered from a kinetic viewpoint, all of the protein crystals so far studied show negative pressure dependencies (Table 1). These inhibitions are due to a decrease in the 2D nucleation rate caused, in the case of a tetragonal hen lysozyme crystal,[14,19] by an increase in the surface free energy of the crystal and, in the case of an orthorhombic hen lysozyme,[23] by an increase in the activation energy for incorporation of the molecules into the crystal. However, since Visuri et al. reported a very drastic acceleration of its crystallization,[3] the glucose isomerase crystal is a good candidate crystal for an investigation of the acceleration of growth kinetics under high pressure. If pressure does have positive effects on growth kinetics, we can use pressure to increase the success rate of crystallization, not only from a thermodynamic viewpoint but also from a kinetic one.

TABLE 1: Pressure Effects on the Solubility and Growth Kinetics of Protein Crystals

protein	solubility	growth kinetics
lysozyme (tetragonal)	increase[4,7,9,10,12,16,19,22]	inhibition[14]
lysozyme (orthorhombic)	decrease[12]	inhibition[23]
subtilisin	increase[13]	inhibition[15]
glucose isomerase	decrease[21]	(this work)

In this work, we measured the growth rate in situ over a wide range of σ under pressures of 0.1 and 100 MPa. Then, to elucidate the kinetic parameter that is responsible for the pressure effect, we compared the observed dependencies of the growth rates on σ with the predictions for a spiral growth model and a 2D nucleation growth model.

2. Experimental Section

Glucose isomerase from *Streptomyces rubiginosus* (D-xylose ketol-isomerase EC 5.3.1.5, 5 times recrystallized, supplied as a crystal suspension by Hampton Research Corp.) was used without further purification.[21] The crystallization solution of glucose isomerase contained 0.91 M ammonium sulfate, 1 mM magnesium sulfate, and 6 mM tris hydrochloride (pH = 7.0). Seed crystals were grown from this solution (glucose isomerase concentration 30 mg mL^{-1} at 10 °C) by a salting-out method.

* To whom correspondence should be addressed. Phone: +81-88-656-7415. Fax: +81-88-655−7025. E-mail: suzuki@chem.tokushima-u.ac.jp.
† The University of Tokushima.
‡ Institute for Materials Research, Tohoku University.
§ Center for Interdisciplinary Research, Tohoku University.

10.1021/jp046419j CCC: $30.25
Published on Web 02/04/2005

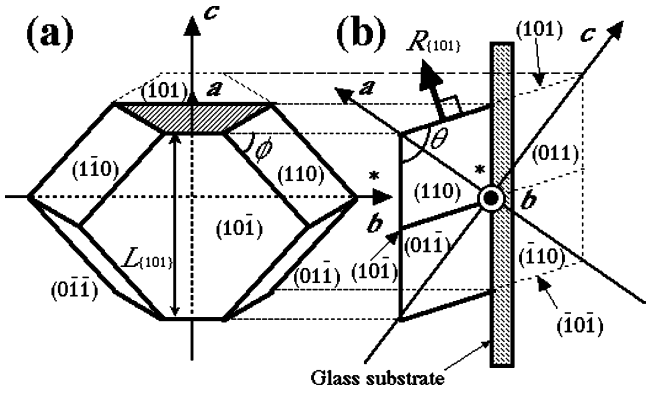

Figure 1. Morphology of a glucose isomerase crystal. (a) Top view and (b) side view. $R_{\{1\ 0\ 1\}}$ shows the growth rate of a {1 0 1} face. $L_{\{1\ 0\ 1\}}$ indicates the distance between the upper and lower sides of a {1 0 1} face. The four (1 0 1), (1 0 $\bar{1}$), ($\bar{1}$ 0 1), and ($\bar{1}$ 0 $\bar{1}$) prism faces are crystallographically equivalent ({1 0 1}).

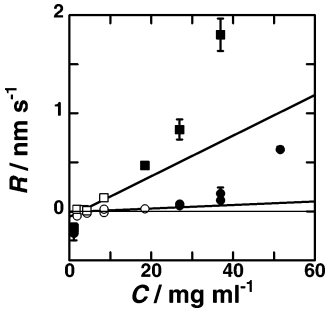

Figure 2. Changes in the growth and dissolution rates of a glucose isomerase crystal as a function of glucose isomerase concentration C under 0.1 (○, ●) and 100 (□, ■) MPa. Since the data show sigmoidal curves, 7 data points for the 0.1 MPa (○) case and 4 points for the 100 (□) MPa were used for the solubility determination. Solid lines indicate the weighted linear fitting lines to the data. Error bars in the vertical axis present the standard deviations derived from the linear fitting of the displacement of the crystal face with time.

The space group of the crystal was $I222$, and the unit cell dimensions were $a = 9.388$ nm, $b = 9.964$ nm, and $c = 10.290$ nm ($Z = 2$).[25] After the preparation of the seed crystals, the crystals and the solution were transferred into an observation cell (made of glass slides) with flexible silicone tubes, and the cell was placed in a high-pressure vessel. The vessel had a pair of transparent sapphire windows for in situ observation under high pressure. Details of the experimental setup were reported in our previous paper.[23]

In this study, the solubilities at 25 °C at 0.1 and 100 MPa were measured more accurately than those in our previous study,[21] since there the errors in the measured solubilities were too large (for instance, $\geq \pm 5$ mg mL^{-1} at 25 °C) to analyze the supersaturation dependence of the growth rates. The growth and dissolution rates of two seed crystals were measured in the range of protein concentrations $C = 1.1-51.1$ mg mL^{-1}. The solubility was defined as the concentration at which the growth and dissolution rates became zero.

3. Results and Discussions

3.1. Morphology of the Crystal. Before measuring the growth and dissolution rates, we determined the face indices of the glucose isomerase crystal from the angles between adjacent faces. As shown in Figure 1, the crystal was bounded by four hexagonal faces and eight parallelogram faces. The space group of the crystal ($I222$) and the symmetry of the morphology indicated that two crystallographic axes had to cross the two ridges of the hexagonal faces (Figure 1a) and that the other axis had to cross the intersection point of the four parallelograms (Figure 1b).

To determine which crystallographic axes correspond to the a, b, and c axes, we measured the angle ϕ prescribed by two ridges of the hexagonal face (Figure 1a). From 26 photomicrographs of the two seed crystals, we determined the average value of ϕ to be $54.0 \pm 0.6°$. We also calculated the angle ϕ for all of the possible combinations of the three crystallographic axes and found three possible correspondences. When the axis indicated by the asterisk in Figure 1a was the a, b, or c axis, the shaded face in Figure 1a became the {0 1 1}, {1 0 1}, or {1 1 0} face, and the values of ϕ could be calculated to be 56.8°, 54.4°, or 53.1°, respectively. From the comparisons of the angles measured and calculated, we concluded that the axis indicated by the asterisk was the b axis, and the face indices were those shown in Figure 1. The four (1 0 1), (1 0 $\bar{1}$), ($\bar{1}$ 0 1), and ($\bar{1}$ 0 $\bar{1}$) prism faces were crystallographically equivalent ({1 0 1} face). Since the {1 0 1} face was the best developed, we measured its growth rate $R_{\{1\ 0\ 1\}}$, defined as the displacement of the {1 0 1} face per second in a direction normal to the {1 0 1} face and expressed as

$$R_{\{101\}} = \frac{\sin\theta}{2} \times \frac{\mathrm{d}L_{\{101\}}}{\mathrm{d}t} \qquad (1)$$

Here $L_{\{1\ 0\ 1\}}$ is the distance between the upper and lower ridges of the {1 0 1} face, and θ, the angle between the (1 0 1) and (1 0 $\bar{1}$) faces, was equal to 95.2°.

3.2. Solubility. We determined the solubilities under pressures of 0.1 and 100 MPa from the concentration at which the growth and dissolution rates of the crystals became zero. To find the concentration, we fitted a linear function of the concentration to seven values of the growth and dissolution rates at 0.1 MPa (○ in Figure 2) and four points at 100 MPa (□ in Figure 2). Error bars in the vertical axis of Figure 2 indicate the standard deviations derived from the linear fitting of the displacement of the crystal face with time.

The solubilities at 25 °C at 0.1 and 100 MPa were determined to be 3.1 ± 0.9 and 2.6 ± 0.5 mg mL^{-1}, respectively (errors of the solubilities were estimated from the errors of the growth and dissolution rates). This result means that the supersaturations of the solutions with the same protein concentrations under pressures of 0.1 and 100 MPa were not much different. Hence, the much larger growth rate at 100 MPa than that at 0.1 MPa (Figure 2) strongly suggests that the acceleration of the crystallization at 25 °C is not due to the pressure effect on the thermodynamics, but is, instead, mainly due to the effect on the growth kinetics.

3.3. Growth Kinetics. The growth rates of the {1 0 1} face of the glucose isomerase crystal were replotted as a function of σ in Figure 3. The error bars in the horizontal axis were estimated from the errors of the solubility at 25 °C.

The growth rate under a pressure of 100 MPa was significantly faster than that at 0.1 MPa. Since, in Figure 3, we compare the growth rates at the same supersaturation level, the increase in the growth rate with pressure is caused solely by the acceleration of the growth kinetics. Since all the protein crystals reported so far show a deceleration of the growth kinetics with increasing pressure (Table 1), the crystallization of glucose isomerase represents the first instance of a pressure-induced acceleration of growth kinetics.

In the case of the growth rates of the {110} and {011} faces, a geometric issue prevented us from measuring them precisely.

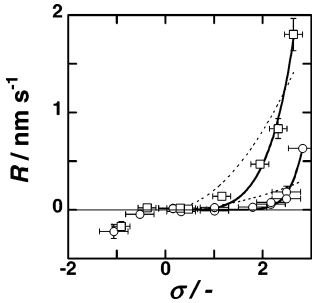

Figure 3. Changes in the growth and dissolution rates as a function of σ under 0.1 (○) and 100 (□) MPa pressure. Solid and dotted curves represent the fitting results obtained by a 2D nucleation growth model of a polynucleation type (eq 3) and a spiral growth model (eq 2), respectively. Error bars in the horizontal axis are estimated from the errors of the solubility at 25 °C.

However, the crystal retained a similar shape during the measurements of the growth rate under high pressure. Evidently, then, the ratios of the growth rate of the {101} face to those of the {110} and {011} faces did not change much with increasing pressure. From this result, we concluded that a rise in pressure also speeded up the growth rates of the {110} and {011} faces.

How does pressure accelerate the growth rate kinetically? The following three hypotheses are conceivable. (1) An increasing pressure reduces the volume of the system, and thus elevates the protein concentration. (2) The rising pressure brings about changes in the crystals' growth mode. (3) Changes in growth parameters such as an activation energy, surface free energy, etc., occur with elevations in pressure.

(1) Elevation of the Protein Concentration through a Reduction in the System Volume. Let us first consider hypothesis (1). Since there is no crystallographic data for the glucose isomerase crystal under high pressure, we can refer to the case of the tetragonal crystal of hen egg-white lysozyme (t-HEWL crystal). How much does the concentration change with increasing pressure? Kundrot and Richards reported that from 0.1 to 100 MPa the volume contraction of the crystal, the solvent in the crystal, and the bulk solution were 1.1, 3.7 and 3.7%,[26,27] respectively. (For that crystal, regardless of the increase in the protein concentration resulting from the volume contraction, the growth kinetics decelerates with increasing pressure.[14]) In the case of the glucose isomerase crystal, the volume contraction of the system is probably on the same order as that of the t-HEWL crystal (i.e., several percent). However, an increase of several percent in the glucose isomerase concentration is too small to explain the drastic acceleration of the growth kinetics shown in Figure 3.

(2) Changes in the Crystals' Growth Mode. To evaluate the second hypothesis, we should first confirm the crystal growth mode under all the growth conditions. Since the crystals observed in this study had clear facets, the crystals formed via a layer-by-layer growth mechanism. Therefore, they must have grown in a spiral growth mode with screw dislocations and/or in a 2D nucleation growth mode.

If the density of the screw dislocations is sufficiently low, the growth rate R of the spiral growth mode is expressed as[28,29]

$$R = \frac{K_s h}{19 f_0 \kappa} \sigma^2 \qquad (2)$$

Here, K_s is a step kinetic coefficient, h a step height, f_0 the area that is occupied by a molecule on the crystal face, and κ a ledge free energy. The fitting results of the R vs σ data with eq 2 are shown as dashed curves in Figure 3. As that figure demonstrates, eq 2 cannot reproduce the experimental data at all.

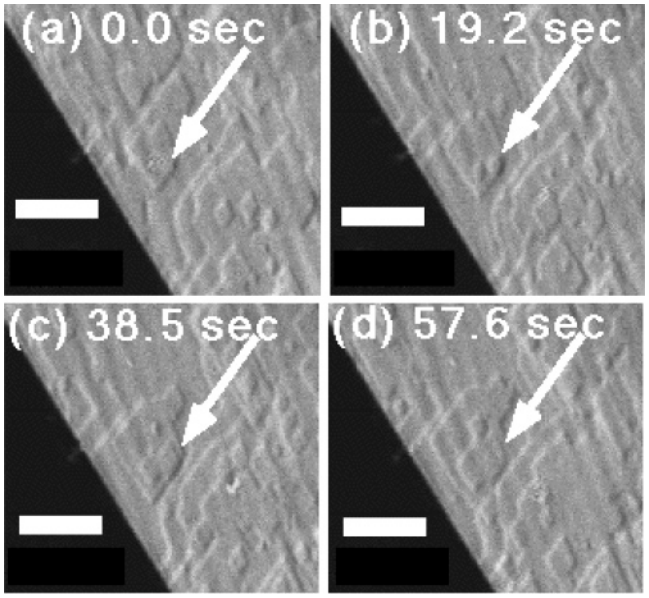

Figure 4. Series of LCM-DIM images of the {1 0 1} face of the glucose isomerase crystal at 0.1 MPa (C = 19.9 mg mL^{-1} and T = 25 °C). Rhombus-shaped 2D islands were formed and spread laterally (see the arrows). The shorter diagonals of the islands are parallel to the ⟨0 1 0⟩ direction of the crystal. The scale bar represents 10 μm. Growth time: 0.0 s (a), 19.2 s (b), 38.5 s (c), and 57.6 s (d).

Next, we take into account the 2D nucleation growth model. Actually, there are two models that can represent the 2D nucleation growth mode: one operating by mononucleation and the other by polynucleation. Through the following reasoning, we judged that the latter is the growth mode in the present case. The growth rate in the mononucleation mode is proportional to the surface area of the relevant face.[30] However, the growth rate of the crystal used in the present study did not depend on the surface area, although two seed crystals of different size ($L_{\{1\ 0\ 1\}} \approx$ 200 and 400 nm) were used. In addition, to confirm the growth mode directly, we observed the surface topography of the {1 0 1} face in situ using a reflection-type laser confocal microscope combined with a differential interference contrast microscope (LCM-DIM system) under atmospheric pressure. Using a LCM-DIM system, Sazaki et al. obtained sufficient contrast to observe in situ elementary growth steps (5.6 nm in height) on the surface of t-HEWL crystals.[31] Figure 4 shows the time course of the LCM-DIM micrographs. The 2D nucleation and subsequent lateral growth of the 2D islands were clearly observable (see the arrows in Figure 4). Thus, we concluded that the glucose isomerase crystal grew in the polynucleation mode.

The growth rate in the polynucleation mode is expressed as[14,23,32,33]

$$R = k_1 \exp\left(\frac{2\sigma}{3}\right)(\exp\sigma - 1)^{2/3}\sigma^{1/6}\exp\left(\frac{-k_2}{\sigma}\right) \qquad (3)$$

where k_1 and k_2 are expressed as

$$k_1 = \left(\frac{\pi}{3}\right)^{1/3} a^{13/3} h^{4/3} \nu \lambda_0^{-2/3} C_e^{4/3} \exp\left(-\frac{\epsilon + \epsilon_{ad} + 2\epsilon_{kink}}{3kT}\right) \qquad (4)$$

TABLE 2: k_1 and k_2 for the Glucose Isomerase Crystals According to Eq 3

	pressure/MPa	
coefficient	0.1	100
k_1/nm s^{-1}	7 ± 6	0.16 ± 0.08
k_2/−	18 ± 2	3 ± 1

and

$$k_2 = \frac{\pi\gamma^2}{3k^2T^2} \tag{5}$$

In eqs 3, 4, and 5, the following symbols are used: a is the distance between the molecules in the crystal; h is the step height; ν is the thermal frequency of a solute; λ_0 is the average distance between the kinks on a step; ϵ is the activation energy for a solute molecule to be incorporated into a critical nucleus; ϵ_{ad} is the activation energy for a solute molecule to be adsorbed on the crystal surface; ϵ_{kink} is the activation energy for a solute molecule to be incorporated into a kink site; γ is the molecular surface energy that represents the excess free energy due to unsatisfied bonds of a molecule at a step edge; and k is the Boltzmann constant. By nonlinear least-squares fitting, eq 3 reproduces the experimental data well, as shown in Figure 3 (solid curves). All experimental data were best fitted to the 2D nucleation growth mode of the polynucleation type. Hence we concluded that there was no change in the growth mode with increasing pressure.

(3) Changes in Growth Parameters. Finally, to consider the third hypothesis, we compared in detail the crystal growth parameters under a pressure of 0.1 MPa with those under 100 MPa. The values obtained for k_1 and k_2 are listed in Table 2. Both of these values for the glucose isomerase crystal decreased with increasing pressure. The decrease in k_1 means a decrease in the growth rate, while the decrease in k_2 promotes an increase in the growth rate. The results shown in Figure 3 indicate that the decrease in k_2 dominated the dependence of the growth rate on pressure. Equation 5 shows that the decrease in k_2 corresponds to the decrease in γ. The evaluated value of the molecular surface energy γ at 100 MPa ($1.8 \pm 0.3\ kT$) is significantly smaller than that at 0.1 MPa ($4.1 \pm 0.3\ kT$). The fall in γ with increasing pressure results in the elevation in the 2D nucleation rate and subsequently the rise in the growth rate; the growth rate of the glucose isomerase crystal is kinetically accelerated with increasing pressure.

How does the γ of the glucose isomerase crystal decrease with increasing pressure? The increase in the number of water molecules hydrating a glucose isomerase molecule (hydration number) could be a candidate mechanism. The variable γ represents the excess free energy due to unsatisfied bonds of the molecule at a step edge. Therefore, the more hydration that occurs at the unsatisfied surface of the protein molecule, the smaller the value of γ that is obtained. However, since there is no structural data for the glucose isomerase molecule under high pressure, let us consider instead the γ of the t-HEWL crystal under high pressure using the high-pressure X-ray crystallographic data that are available for this molecule. For that crystal, the study of its growth kinetics under high pressure revealed that the γ of the t-HEWL crystal increased with increasing pressure,[14] a result contrary to that for the γ of the glucose isomerase crystal. This increase in γ probably means a reduction with rising pressure in the hydration number of a lysozyme molecule in the t-HEWL crystal. In addition, Kundrot et al. investigated the structure of the lysozyme molecules in the t-HEWL crystal under 100 MPa pressure by X-ray crystallography and found that, at this high pressure, the number of hydrogen bonds made per Å^2 of the lysozyme molecule's polar accessible surface area was 7% fewer than that at 0.1 MPa.[26,27] This decrease in the number of the hydrogen bonds strongly supports the decrease in the hydration number and the consequent increase in γ.

To confirm our use of the hydration number as an explanation for the γ values, a high-pressure X-ray analysis of the glucose isomerase crystal is indispensable. Although several high-pressure crystallographic studies have been carried out so far,[26,27,34−39] no one has yet performed an in situ X-ray analysis under high pressure using a crystal nucleated and grown under high pressure. Kundrot and Richards were first to analyze the structure of the lysozyme molecule by in situ X-ray analysis under high pressure, using a crystal grown under atmospheric pressure.[26,27,34] However, the deformation of the molecule in the crystal with increasing pressure was different from that in the solution. Using NMR, Rafaee et al. have found a large β-domain deformation of a lysozyme molecule in solution,[40] whereas such a deformation was not mentioned in Kundrot's report.[26,27] Therefore, we are now planning to collect diffraction data in situ using a glucose isomerase crystal that crystallized under high pressure. The precise 3D structure of the protein molecules under high pressure will reveal the effects of pressure on the hydration number (i.e., γ), as well as the intermolecular interaction in the crystal.[41−43] Such a collection of in situ diffraction data will also enable us to evaluate the effects of pressure on the quality of the protein crystals.

In this work, we found that pressure could accelerate the crystallization of glucose isomerase. With increasing pressure, the growth rates of these crystals were speeded up both thermodynamically and kinetically. Thus, pressure can probably enhance the yield of protein crystals suitable for X-ray structure analysis.

4. Conclusions

In this study, we measured, in situ, the growth and dissolution rates of the {1 0 1} face of the glucose isomerase crystal under 0.1 and 100 MPa of pressure. Our key findings are as follows.

(1) The solubilities of the glucose isomerase crystals at 25 °C under 0.1 and 100 MPa were 3.1 ± 0.9 and 2.6 ± 0.5 mg mL^{-1}, respectively.

(2) We have found the first instance of a case in which the growth kinetics of protein crystals can be accelerated with increasing pressure.

(3) The supersaturation dependence of the growth rate of the glucose isomerase crystal agreed well with a polynucleation type of 2D nucleation growth model. This curve fitting strongly suggested that the acceleration of the growth kinetics with pressure was due to a decrease in the molecular surface energy γ.

Acknowledgment. This study was carried out as a part of "Program for an improvement of education" promoted by the University of Tokushima. This work was partially supported by Grants-in-Aid (No. 16760014 (Y. S.) and Nos. 12750006 and 16360001 (G. S.)) of Scientific Research of the Ministry of Education, Culture, Sports, Science, and Technology Japan. This work was performed under the inter-university cooperative research program of the Institute for Materials Research, Tohoku University.

References and Notes

(1) HYPERLINK http://proteome.bnl.gov/; http://proteome.bnl.gov/.
(2) Chayen, N. E.; Saridakis, E. *Acta Crystallogr.* **2002**, *D58*, 921−927.
(3) Visuri, K.; Kaipainen, E.; Kivimaki, J.; Niemi, H.; Leisola, M.; Palosaari, S. *Bio/Technology* **1990**, *8*, 547−549.
(4) Gross, M.; Jaenicke, R. *FEBS Lett.* **1991**, *284*, 87−90.
(5) Gross, M.; Jaenicke, R. *Biophys. Chem.* **1993**, *45*, 245−252.
(6) Schall, C. A.; Wiencek, J. M.; Yarmush, M.; Arnold, E. *J. Cryst. Growth* **1994**, *135*, 548−554.
(7) Suzuki, Y.; Miyashita, S.; Komatsu, H.; Sato, K.; Yagi, T. *Jpn. J. Appl. Phys.* **1994**, *33*, L1568-L1570.
(8) Saikumar, M. V.; Glatz, C. E.; Larson, M. A. *J. Cryst. Growth* **1995**, *151*, 173−179.
(9) Lorber, B.; Jenner, G.; Giege, R. *J. Cryst. Growth* **1996**, *158*, 103−117.
(10) Takano, K. J.; Harigae, H.; Kawamura, Y.; Ataka, M. *J. Cryst. Growth* **1997**, *171*, 554−558.
(11) Saikumar, M. V.; Glatz, C. E.; Larson, M. A. *J. Cryst. Growth* **1998**, *187*, 277−288.
(12) Sazaki, G.; Nagatoshi, Y.; Suzuki, Y.; Durbin, S. D.; Miyashita, S.; Nakada, T.; Komatsu, H. *J. Cryst. Growth* **1999**, *196*, 204−209.
(13) Webb, J. N.; Waghmare, R. Y.; Carpenter, J. F.; Glatz, C. E.; Randolph, T. W. *J. Cryst. Growth* **1999**, *205*, 563−574.
(14) Suzuki, Y.; Miyashita, S.; Sazaki, G.; Nakada, T.; Sawada, T.; Komatsu, H. *J. Cryst. Growth* **2000**, *208*, 638−644.
(15) Waghmare, R. Y.; Webb, J. N.; Randolph, T. W.; Larson, M. A.; Glatz, C. E. *J. Cryst. Growth* **2000**, *208*, 678−686.
(16) Suzuki, Y.; Sawada, T.; Miyashita, S.; Komatsu, H.; Sazaki, G.; Nakada, T. *J. Cryst. Growth* **2000**, *209*, 1018−1022.
(17) Logtenberg, E. H. P.; Meersman, F.; Rubens, P.; Heremans, K.; Frank, J. *High-Pressure Res.* **2000**, *19*, 675−680.
(18) Waghmare, R. Y.; Pan, X. J.; Glatz, C. E. *J. Cryst. Growth* **2000**, *210*, 746−752.
(19) Suzuki, Y.; Sazaki, G.; Miyashita, S.; Sawada, T.; Tamura, K.; Komatsu, H. *Biochim. Biophys. Acta* **2002**, *1595*, 345−356.
(20) Pan, X.; Glatz, C. E. *Cryst. Growth Des.* **2002**, *2*, 45−50.
(21) Suzuki, Y.; Sazaki, G.; Visuri, K.; Tamura, K.; Nakajima, K.; Yanagiya, S. *Cryst. Growth Des.* **2002**, *2*, 321−324.
(22) Kadri, A.; Lorber, B.; Jenner, G.; Giege, R. *J. Cryst. Growth* **2002**, *245*, 109−120.
(23) Nagatoshi, Y.; Sazaki, G.; Suzuki, Y.; Miyashita, S.; Ujihara, T.; Fujiwara, K.; Usami, N.; Nakajima, K. *J. Cryst. Growth* **2003**, *254*, 188−195.
(24) van Hook, W. A. *Fluid Phase Equilib.* **1980**, *4*, 287−292.
(25) Carrell, H. L.; Glusker, J. P.; Burger, V.; Manfre, F.; Tritsch, D.; Biellmann, J.-F. *Proc. Natl. Acad. Sci. U.S.A.* **1989**, *86*, 4440−4444.
(26) Kundrot, C. E.; Richards, F. M. *J. Mol. Biol.* **1987**, *193*, 157−170.
(27) Kundrot, C. E.; Richards, F. M. *J. Mol. Biol.* **1988**, *200*, 401−410.
(28) Burton, W. K.; Cabrera, N.; Frank, F. C. *Philos. Trans. Royal Soc. London A* **1951**, *243*, 299−358.
(29) Cabrera, N.; Levine, M. M. *Philos. Mag.* **1956**, *1*, 450−458.
(30) Becker, R.; Doring, W. *Ann. Phys.* **1935**, *24*, 719−752.
(31) Sazaki, G.; Matsui, T.; Tsukamoto, K.; Usami, N.; Ujihara, T.; Fujiwara, K.; Nakajima, K. *J. Cryst. Growth* **2004**, *262*, 536−542.
(32) Kurihara, K.; Miyashita, S.; Sazaki, G.; Nakada, T.; Suzuki, Y.; Komatsu, H. *J. Cryst. Growth* **1996**, *166*, 904−908.
(33) Malkin, A. I.; Chernov, A. A.; Alexeev, I. V. *J. Cryst. Growth* **1989**, *97*, 765−769.
(34) Kundrot, C. E.; Richards, F. M. *J. Appl. Crystallogr.* **1986**, *19*, 208−213.
(35) Katrusiak, A. *High Pressure Res.* **1991**, *6*, 155−167.
(36) Katrusiak, A.; Dauter, Z. *Acta Crystallogr. D* **1996**, *52*, 607−608.
(37) Fourme, R.; Kahn, R.; Mezouar, M.; Girard, E.; Hoerentrup, C.; Prange, T.; Ascone, I. J. *Synchrotron Rad.* **2001**, *8*, 1149−1156.
(38) Urayama, P.; Philips, G. N., Jr.; Gruner, S. M. *Structure* **2002**, *10*, 51−60.
(39) Fourme, R.; Ascone, I.; Kahn, R.; Mezouar, M.; Bouvier, P.; Girard, E.; Lin, T.; Johnson, J. E. *Structure* **2002**, *10*, 1409−1414.
(40) Rafaee, M.; Tezuka, T.; Akasaka, K.; Williamson, M. P. *J. Mol. Biol.* **2003**, *327*, 857−865.
(41) Oki, H.; Matsuura, Y.; Komatsu, H.; Chernov, A. A. *Acta Crystallogr. D* **1999**, *55*, 114−121.
(42) Hondoh, H.; Sazaki, G.; Miyashita, S.; Durbin, S. D.; Nakajima, K.; Matsuura, Y. *Cryst. Growth Des.* **2002**, *1*, 327−332.
(43) Matsuura, Y.; Chernov, A. A. *Acta Crystallogr. D* **2003**, *59*, 1347−1356.